

A New Compact Rectangle-Like Slot Antenna with WiMAX and WLAN Rejection

M. Akbari*¹, M. Khodaei³, S. Zarbakhsh¹, and Abdelrazik Sebak²

¹ Young Researchers and Elite Club
Central Tehran Branch, Islamic Azad University, Tehran, Iran
*akbari.telecom@gmail.com, mo_akba@encs.concordia.ca

² Electrical and Computer Department
Concordia University, Quebec H3G 1M8, Canada

³ Faculty of Eng., Department of Electrical Engineering
Shahid Beheshti University, Tehran, Iran

Abstract — In this manuscript, a new CPW-fed slot antenna with two band-notches for ultra-wideband communication systems is proposed. The antenna contains a trapezoid-shaped patch and a slotted ground plane. To achieve two notched bands, both of the inverted L-shaped strip and triangle-shaped element connecting to patch by via are used. The designed antenna is printed on an FR4 substrate with compact size of 20×27 mm². Moreover, the antenna has been successfully fabricated and measured, indicating extended impedance bandwidth (3–11.2 GHz, VSWR≤2) and dual band-notched (3.2–3.9 GHz and 5–5.9 GHz) respectively.

Index Terms — Coplanar waveguide (CPW) antennas, notched band, ultra wideband (UWB).

I. INTRODUCTION

In recent years, planar structures or printed antennas have attracted much attention due to the set of benefits including simple structure, low profile, easy integration with monolithic microwave integrated circuits (MMICs), and ease of fabrication. In spite of all these advantages, the narrow impedance bandwidth is one of the main challenges of antenna design. Newly, various techniques have been proposed to overcome the narrow bandwidth of these antennas. A big number of antennas with different structures have been experimentally characterized which patch of this type of reported antennas has different shapes such

as rectangular, Disc, triangle and oval forms [1-2]. There are many techniques that contain changes in configuration and geometry of patch, feed line, and ground structure which is introduced as the most important of all to enhance the bandwidth and access to UWB bandwidth [3-4]. On the other hand, the frequency range for UWB systems between 3.1 and 10.6 GHz will end up interfering to the existing wireless communication systems, such as the wireless local area network (WLAN) for IEEE 802.11a operating at 5.15–5.35 and 5.725–5.825 GHz, the IEEE 802.16 WiMAX system at 3.3–3.69, 5.25–5.85 GHz; therefore, the UWB antenna with a band-stop performance is needed. For this goal, different techniques with single, dual, and multiple notch functions have been recently reported [5-6]. In this paper, a novel rectangle-like slot antenna with wide impedance bandwidth and dual band-notched characteristic is proposed. By employing both triangle-shaped coupling element and an inverted L-shaped strip, dual band-notch function can be achieved at the central frequencies 3.5 and 5.5 GHz.

II. ANTENNA DESIGN

The configuration and photo of the fabricated antenna are shown in Fig. 1, the proposed antenna has a compact size 20×27 mm² which is printed on a FR4 substrate with thickness 1.6 mm and permittivity 4.4. Only reason for using FR4 is its cheap cost. The width of the CPW feedline, W_f , and

the gap between the ground and feedline, g , are fixed at 2.6 and 0.4 mm respectively. The basic antenna structure contains a trapezoid-shaped patch and a slotted ground plane. As illustrated in Fig. 1, the rectangle-like slot of the ground plane has a width $W1$ and length $L1$ and the proposed antenna is connected to a 50Ω SMA connector for signal transmission. To achieve two notched bands has been used two different techniques, the former an inverted L-shaped strip for filtering 3.2 up to 3.9 GHz, the latter triangle-shaped coupling element on the back side which is connected to patch by a via for generating another notch from 5 up to 5.9 GHz, that both of them seem to be very sharp which will be more examined as follows.

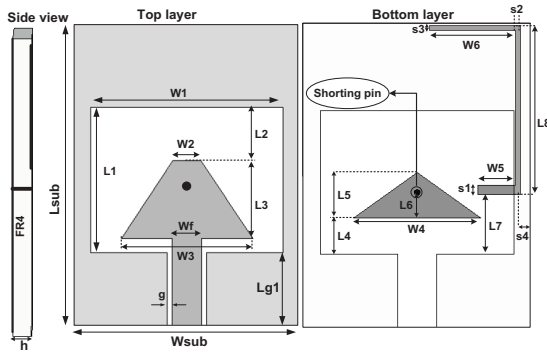


Fig. 1. Geometry of the fabricated antenna.

III. ANTENNA PERFORMANCE AND DISCUSSION

A. Time-domain analysis

Computation of the dispersion that occurs when the antenna radiates a pulse signal is also of interest. The transmit transfer functions of the antennas were used to compute the radiated pulse in different directions when a reference signal was applied at the antenna input. This signal should present an UWB spectrum covering the antenna bandwidth and particularly the FCC mask from 3.1 to 10.6 GHz. It is shown in Fig. 2 an acceptable approximation to a FCC mask compliant pulse can be obtained with a Gaussian seventh derivative. This pulse is represented in the time domain by:

$$G(t) = A \cdot \exp\left(\frac{-t^2}{2\delta^2}\right), \quad (1)$$

$$G^n(t) = \frac{d^n G}{dt^n} = (-1)^n \frac{1}{(\sqrt{2}\delta)^2} \cdot H_n\left(\frac{t}{\sqrt{2}\delta}\right) \cdot G(t), \quad (2)$$

$$H_7(t) = 128t^7 - 1344t^5 + 3360t^3 - 1680t. \quad (3)$$

This signal and its spectrum are represented in Fig. 2. The pulse bandwidth is exactly into mask desired. Luckily, after drawing various Gaussian pulses from the first to eighth derivative, it was obtained that the best pulse for covering FCC mask can be the seventh derivative. Besides, with a bit of tolerance, the sixth and eighth derivative are acceptable. In telecommunications systems, the correlation between the transmitted (TX) and received (RX) signals is evaluated using the fidelity factor (4):

$$F = \max_{\tau} \left| \frac{\int_{-\infty}^{+\infty} S(t)r(t-\tau)dt}{\sqrt{\int_{-\infty}^{+\infty} S(t)^2 \cdot \int_{-\infty}^{+\infty} r(t)^2 dt}} \right|, \quad (4)$$

where $S(t)$ and $r(t)$ are the TX and RX signals, respectively. For impulse radio in UWB communications, it is necessary to have a high degree of correlation between the TX and RX signals to avoid losing the modulated information. However, for most other telecommunication systems, the fidelity parameter is not that relevant. In order to evaluate the pulse transmission characteristics of the proposed antenna in the case of without notch, two configurations (side-by-side and face-to-face orientations) were chosen. The transmitting and receiving antennas were placed in a $d=25$ cm distance from each other [7]. As shown in Figs. 3 and 4, although the received pulses in each of two orientations are broadened, a relatively good similarity exists between the RX and TX pulses. Using (4), the fidelity factor for the face-to-face and side-by-side configurations was obtained equal to 0.94 and nearly 0.96 in order. These values for the fidelity factor show that the antenna imposes negligible effects on the transmitted pulses. The pulse transmission results are obtained using CST [8].

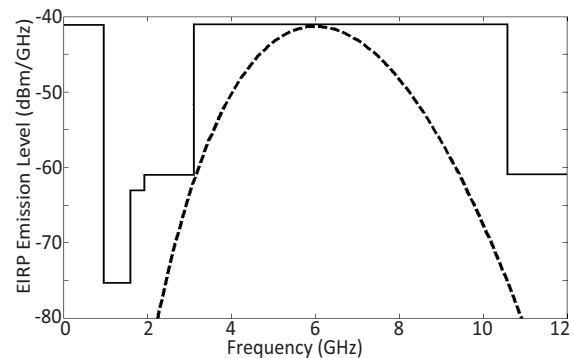


Fig. 2. Power spectrum density compared to FCC mask.

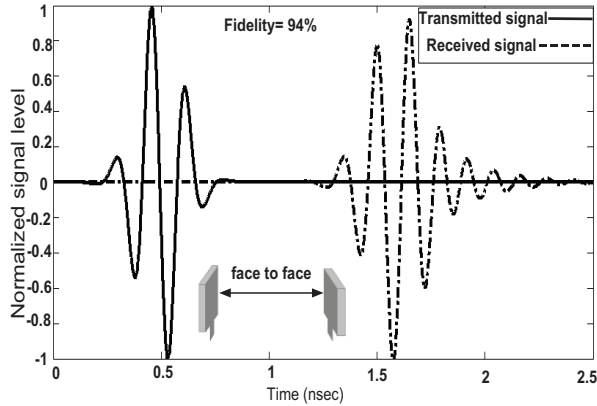


Fig. 3. Transmitted and received pulses in time domain for a UWB link with identical antennas without notches in face-to-face orientation.

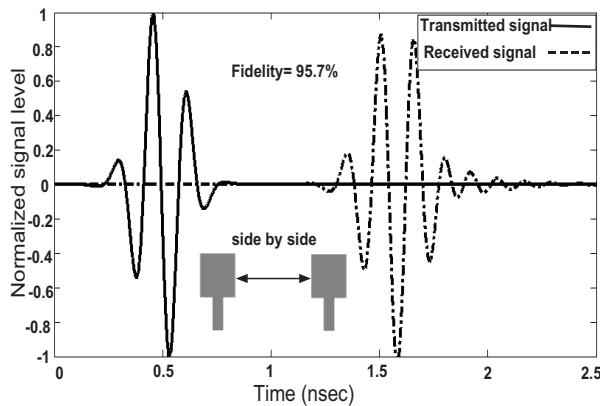


Fig. 4. Transmitted and received pulses in time domain for a UWB link with identical antennas without notches in side by side orientation.

B. Frequency-domain analysis

In UWB systems, the information is transmitted using short pulses. Therefore, it is important to study the temporal behavior of the transmitted pulse. The communication system for UWB pulse transmission must limit distortion, spreading and disturbance as much as possible. Group delay is an important parameter in UWB communication, which represents the degree of distortion of pulse signal. The key in UWB antenna design is to obtain a good linearity of the phase of the radiated field because the antenna should be able to transmit the electrical pulse with minimal distortion. Usually, the group delay is used to evaluate the phase response of the transfer function because it is

defined as the rate of change of the total phase shift with respect to angular frequency. Ideally, when the phase response is strictly linear, the group delay is constant;

$$\text{group delay} = \frac{-d\theta(\omega)}{d\omega} \tag{5}$$

As depicted from Fig. 5, the group delay variation for the antenna is presented, which its variation is approximately flat and less than 0.6ns over the frequency band of interest; except dual notched bands, which ensure us pulse transmitted or received by the antenna will not distort seriously and will retain its shape. Hence, the antenna is useful for modern UWB communication systems. Phase S21 for face to face and side by side orientations are also illustrated in Figs. 6 and 7. As previously expected, the plot shows a linear variation of phase in the total operating band except stop bands. It is important to note again, that the distance between both the identical antennas in face to face and side by side orientations is 25 cm which has been extracted from [7]. In the following, the square antenna with different parameters were constructed, and the numerical and experimental results of the input impedance and radiation characteristics are presented and discussed. Triangle-shaped coupling element which is connected to patch by via, and the proposed antenna. Meanwhile, Fig. 8 also illustrates the antenna topology. VSWR (voltage standing wave ratio) characteristics for three antennas mentioned in Fig. 8 are exhibited in Fig. 9. The simulated results are achieved using the Ansoft simulation software high-frequency structure simulator [9].

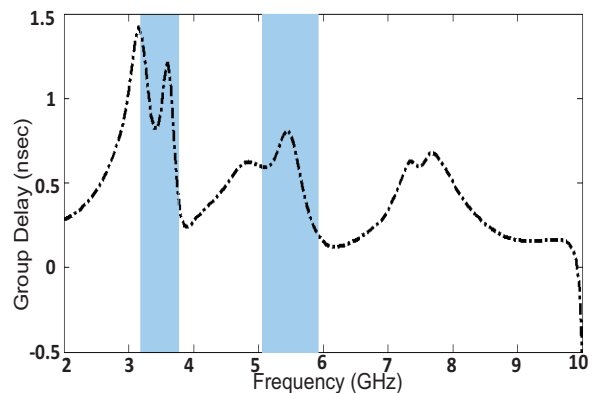


Fig. 5. Group delay of the antenna.

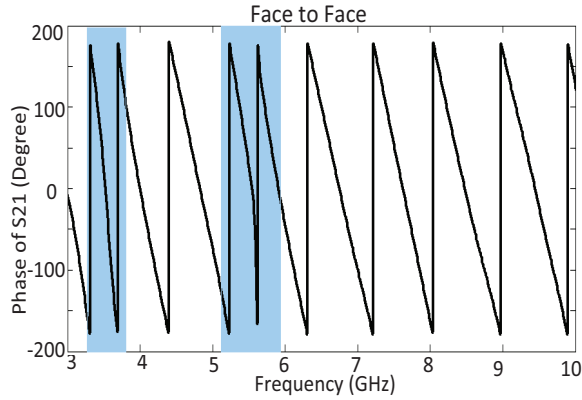


Fig. 6. Simulated phase S21 with a pair of identical antennas for face to face orientation.

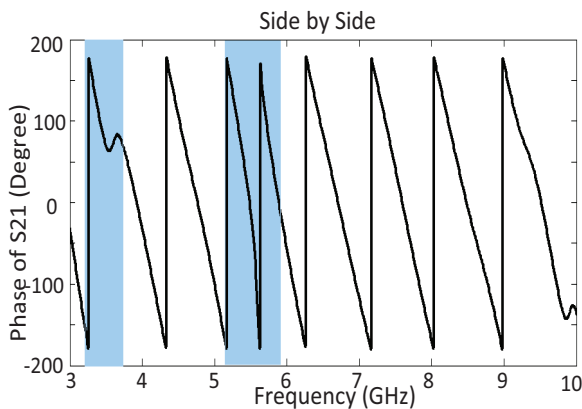


Fig. 7. Simulated phase S21 with a pair of identical antennas for side by side orientation.

The optimal dimensions of the antenna are demonstrated in Table 1. Figure 8 displays the structure of the different slot antennas including: (a) the simple slot antenna without notched bands, (b) the slot antenna with triangle-shaped coupling element and via, and (c) proposed antenna. According to it, by using triangle-shaped coupling element, which is connected to patch by a via shown in Fig. 8 (b), the antenna can filter the WLAN interference band from 5 up to 5.9 GHz. Moreover, the inverted L-shaped strip on the back side, shown in Fig. 8 (c), can create another notched band from 3.2 up to 3.9 GHz. There is an interesting point to note, both of the notched bands obtained are approximately sharp and independent from each other. It means that they have no effect on each other. As depicted in Fig. 10, parameter W6 has a noticeable influence on frequency shifting. With regard to it, with increasing length W6, the center frequency is decreased regularly in a way that with

rising 1.5 mm in length W6 centre frequency of the notched band is reduced about 0.5 GHz.

Table 1: Optimal dimensions of the antenna

Wsub	Lsub	h	Wf	W1	W2	W3	W4
20	27	1.6	2.6	16.8	2.4	11.5	11
W5	W6	L1	L2	L3	L4	L5	L6
3.3	7.5	12.7	4.6	6.9	3.2	4	2.25
L7	L8	Lg1	g	S1	S2	S3	S4
5.3	14.9	6.6	0.4	0.8	0.4	0.4	1

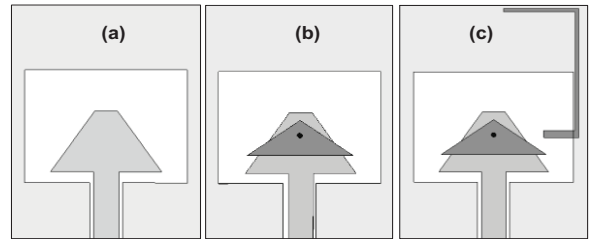


Fig. 8. (a) The simple slot antenna without notched bands, (b) The slot antenna with triangle-shaped element and via, and (c) the proposed antenna.

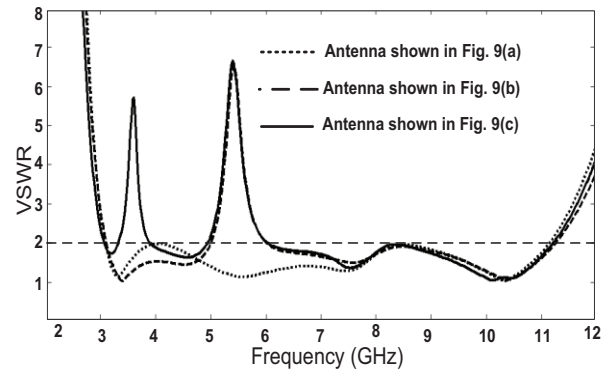


Fig. 9. Simulated VSWR characteristics for antennas shown in Fig. 8.

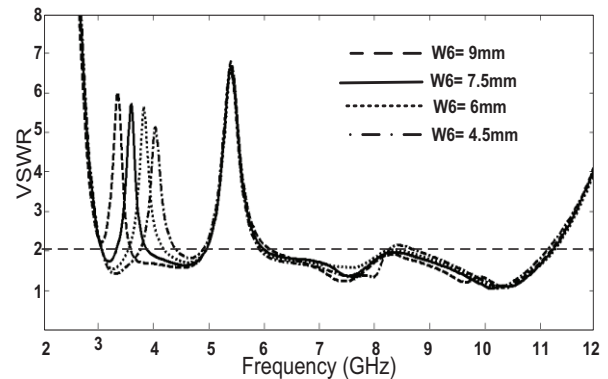


Fig. 10. VSWR characteristics for the antenna with different values W6.

The best value W_6 for covering 5.15 to 5.85 corresponds to 7.5 mm. As mentioned before, in this study to generate the band-stop performance on WiMAX band with center frequency 5.5 GHz, is used a triangle-shaped coupling element, which is connected to patch by via. The simulated VSWR curves with different values W_4 are plotted in Fig. 11. As exhibited in Fig. 11, when the length W_4 increases gradually, center frequency of the notched band is diminished steadily.

Thus, the optimized W_4 is 11 mm. From these results, it can be found that the notch frequencies are controllable by changing the lengths W_6 and W_4 . The proposed antenna was fabricated and tested in the Antenna Measurement Laboratory at Iran Telecommunication Research Center.

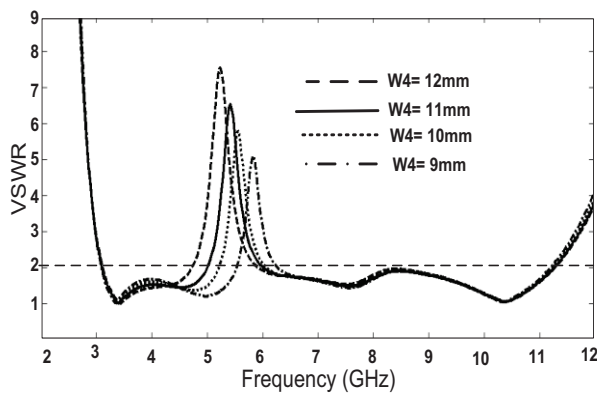


Fig. 11. Simulated VSWR characteristics of the antenna with triangle-shaped element and via with different values W_4 .

It can also be observed in Fig. 12 (a), by using the triangle-shaped element, the current at 5.5 GHz is more concentrated on it and via. On the other hand, Fig. 12 (b) depicts the current distribution at 3.5 GHz in a way that most current is seen on L-shaped strip indicating its effect in creating the second notched band at centre frequency 3.5 GHz. Figure 13 exhibits the measured and simulated VSWR characteristics of the antenna. The fabricated antenna can cover the frequency band from 3 to 11.2 GHz. The antenna has a compact size of $20 \times 27 \text{ mm}^2$, whereas showing the band rejection performance in the frequency bands of 3.2 up to 3.9 GHz and 5 to 5.9 GHz, respectively. As illustrated in Fig. 13, there is a discrepancy between measured result and simulated data, it is more likely due to the effect of the SMA port. The return loss of the

antenna has been measured using an Agilent E8362B network analyzer in its full operational span (10 MHz–20 GHz).

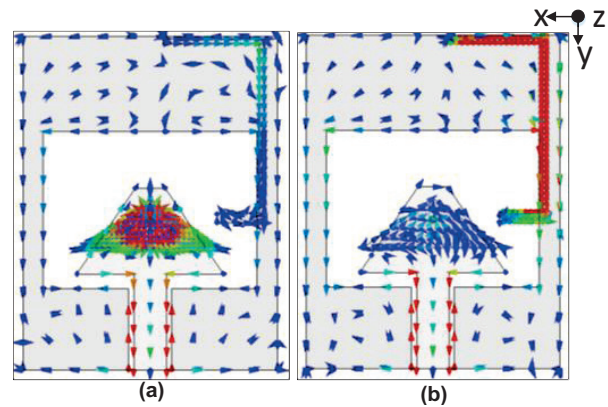


Fig. 12. Simulated current distributions: (a) on the triangle-shaped element and via at 5.5 GHz, and (b) on L-shaped strip at 3.5 GHz.

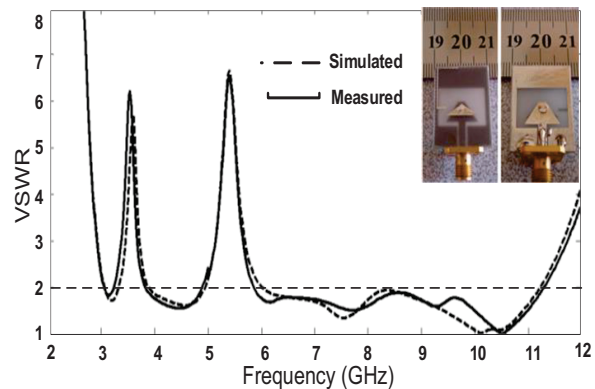


Fig. 13. Measured and simulated VSWR characteristics for the antenna.

Figure 14 shows the measured gain of the antenna with and without stop bands. A sharp fall in gain of the antenna at the centre frequencies of notched bands 3.5, 5.5 GHz, is seen. For other frequencies outside the notched frequency bands, the antenna gain with notch is similar to those without it. Figure 15 depicts the radiation patterns including the co-polarization and cross-polarization in the H-plane ($x-z$ plane) and E-plane ($y-z$ plane) at two frequencies 4.5 GHz and 9 GHz. It can be observed that the radiation patterns in $x-z$ plane are nearly omnidirectional for the two frequencies while radiation patterns in $y-z$ plane or E-plane are about dipole-like shape.

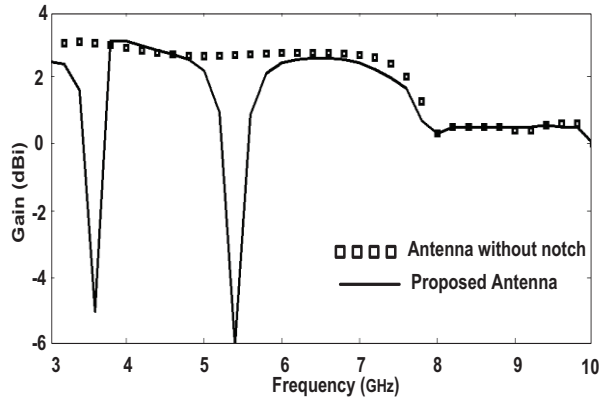


Fig. 14. Measured gain of the antenna without and with notched bands.

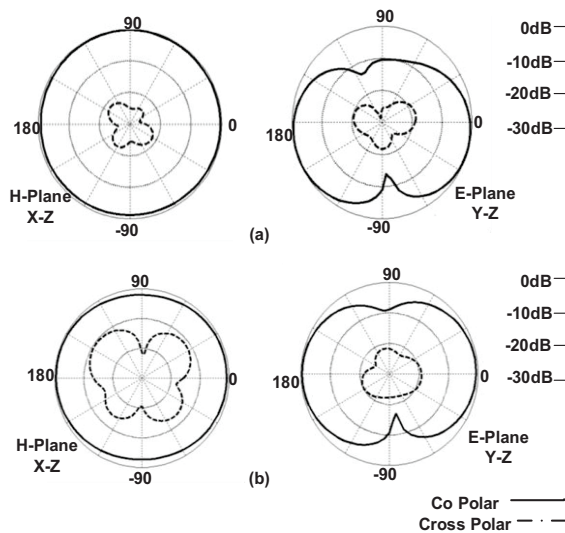


Fig. 15. Radiation patterns of the antenna at: (a) 4.5 GHz and (b) 9 GHz.

IV. CONCLUSION

In this paper, a new CPW antenna with capability of broad impedance bandwidth for UWB applications is presented. The antenna can cover impedance bandwidth from 3 to 11.2 GHz with $VSWR \leq 2$ and indicates a good omnidirectional radiation pattern even at higher frequencies. The antenna has a compact size of $20 \times 27 \text{ mm}^2$ while exhibiting the band stop performance in the frequency bands from 3.2 to 3.9 GHz and 5 up to 5.9 GHz, respectively. Simulated and experimental

results exhibits that the antenna could be a good candidate for UWB application.

REFERENCES

- [1] J.-H. Lu and C.-H. Yeh, "Planar broadband arch-shaped monopole antenna for UWB system," *IEEE Transactions on Antennas and Propagation*, vol. 60, no. 7, pp. 3091-3095, 2012.
- [2] C.-C. Lin, Y.-C. Kan, L.-C. Kuo, and H.-R. Chuang, "A planar triangular monopole antenna for UWB communication," *IEEE Microwave and Wireless Components Letters*, vol. 15, no. 10, pp. 624-626, 2005.
- [3] M. Mighani, M. Akbari, and N. Felegari, "A novel SWB small rhombic microstrip antenna with parasitic rectangle into slot of the feed line," *Applied Computational Electromagnetics Society (ACES) Journal*, vol. 27, no. 1, pp. 74-79, January 2012.
- [4] R. Zaker, C. Ghobadi, and J. Nourinia, "Bandwidth enhancement of novel compact single and dual band-notched printed monopole antenna with a pair of L-shaped slots," *IEEE Transactions on Antennas and Propagation*, vol. 57, no. 12, 2009.
- [5] R. Emadian, M. Mirmozafari, C. Ghobadi, and J. Nourinia, "Bandwidth enhancement of dual band-notched circle-like slot antenna," *Electronics Letters*, vol. 48, no. 7, pp. 356-357, March 2012.
- [6] M. Mighani, M. Akbari, and N. Felegari, "A CPW dual band notched UWB antenna," *Applied Computational Electromagnetics Society (ACES) Journal*, vol. 27, no. 4, pp. 352-359, April 2012.
- [7] C. R. Medeiros, J. R. Costa, and C. A. Fernandes, "Compact tapered slot UWB antenna with WLAN band rejection," *IEEE Antennas and Wireless Propagation Letters*, vol. 8, pp. 661-664, 2009.
- [8] CST Microwave Studio, ver. 2008. Computer Simulation Technology, Framingham, MA, 2008.
- [9] Ansoft HFSS User's Manual, Ansoft Corporation, Beta Release 11.0, April 2007.